

Comparative analysis of microstructure evolution and magnetic properties in strip-cast vs. Conventionally produced non-grain-oriented electrical steel

Dorothea Czempas^{1,a*}, Sebastian Häner^{1,b}, Max Müller^{1,c},
David Bailly^{1,d} and Emad Scharifi^{1,e}

¹Institute of Metal Forming (IBF), RWTH Aachen University, 52072 Aachen, Germany

^adorothea.czempas@ibf.rwth-aachen.de, ^bsebastian.haener@ibf.rwth-aachen.de,

^cmax.mueller@ibf.rwth-aachen.de, ^ddavid.bailly@ibf.rwth-aachen.de,

^eemad.scharifi@ibf.rwth-aachen.de

Keywords: Twin-Roll Casting, Non-Oriented Electrical Steel, Magnetic Properties, Microstructure

Abstract. Non-grain-oriented electrical steels are essential for motors and generators, requiring high magnetic induction and low iron losses. Magnetic properties are influenced by grain size, texture, thickness, and alloying content. Twin-roll casting (TRC) efficiently produces FeSi alloys as near-net strips, eliminating hot rolling and reducing costs, emissions, and energy. Despite its economic and magnetic advantages, understanding TRC's impact on microstructure and processing into electrical steel remains limited. This study investigates the microstructural evolution and magnetic properties of a Fe-2.9Si-1.35Al alloy processed via TRC (1.6 mm thickness) and further refined through warm rolling, cold rolling, and annealing to produce 0.27 mm NGO steel. Results, including Electron Backscatter Diffraction analysis and single-sheet testing, are compared to conventionally processed hot-strip material. Findings show that TRC with proper processing adjustments enables the production of magnetic properties comparable to industrial materials, though differences arise from grain morphology and texture. Key findings: TRC material exhibits better polarization due to its favorable texture; Loss performance is inferior, likely due to inhomogeneous grain size distribution.

Introduction

Non-grain-oriented (NGO) electrical steels are essential for applications in electric motors and generators, where they serve as core materials. These steels require high magnetic induction and low iron loss to achieve energy-efficient performance. Key factors determining their magnetic properties include grain size, crystallographic texture, sheet thickness, and alloying content, particularly silicon and aluminum. The twin-roll casting (TRC) process has emerged as an efficient method for producing FeSi alloys, enabling near-net-shape strips with thicknesses of 1–5 mm directly from the melt. By eliminating the need for hot rolling, this process reduces costs, emissions, energy consumption, and production time [1]. In addition to these economic advantages, TRC can generate a magnetically favorable texture in the as-cast material [2], [3]. Optimizing the texture and microstructure of electrical steels is critical to achieving superior magnetic properties. In body-centered cubic (BCC) silicon steels, a {100} crystallographic texture is particularly desirable because the <001> direction corresponds to the easy magnetization axis [4]. However, conventional processing techniques often induce a pronounced γ -fiber ($\{111\}/\text{ND}$) texture due to the extensive deformation during hot and cold rolling, which can detrimentally affect magnetic properties [5], [6]. In contrast, the strip casting process offers a novel approach to enhancing magnetic performance by increasing the fraction of favorable textures while preserving the as-cast microstructure with minimal deformation [7]. Additionally to texture, controlling grain



size is vital, as an optimal grain size minimizes core losses in specific Fe-Si alloys [8], [9]. Despite these advantages, the understanding of TRC-produced strips, particularly their as-cast microstructure and subsequent processing into electrical steel, remains incomplete due to limited studies and inconsistent data [10]. The aim of the present study is to contribute to the detailed understanding of how the process applied affects the microstructural characteristics, in particular grain size distribution and texture, compared to the conventionally produced material – slab-casted and hot rolled – of the same alloy. This work focuses on correlating the evolution of these microstructural characteristics from strip casting and conventional hot-strip to the fully finished electrical sheet. Therefore, a Fe-2.9Si-1.35Al alloy was produced by TRC with a thickness of 1.6 mm and further processed by warm rolling, cold rolling, and final annealing into an NGO electrical steel of 0.27 mm thickness as depicted in Fig. 1. Furthermore, the resulting magnetic properties are examined with regard to the grain morphologies and textures. The findings are compared to equivalently processed hot-strip of the same alloy in order to show that by adapting the further processing after TRC, comparable values to the industrial material can be achieved.

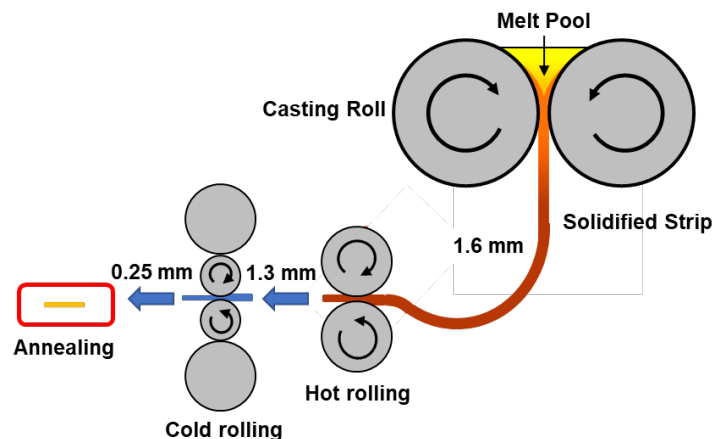


Figure 1 – Schematic view of the twin-roll casting process, rolling and annealing

Material and Methods

Strip casting, rolling and final annealing. A Fe-2.9Si-1.35Al-0.18Mn iron alloy was cast via TRC with a thickness of 1.6 mm on the twin roll caster at the Institute of Metal Forming (IBF) of RWTH Aachen University. For this, 150 kg of the alloy were smelted in an induction furnace and poured via a refractory channel system and a tundish between the two counter rotating rolls of 150 mm width. To inert the pool and control the heat transfer between the casting rolls and the strip shells, the melt pool was shrouded with argon gas. A more detailed description of the process was done by Daamen et al. [11]. The casted strip was further processed by one pass of hot rolling at 1100 °C with a pass reduction of approximately 20 %. This step is used to recreate inline hot rolling after strip casting, which was not possible on the equipment, and is intended to eliminate the casting microstructure and close any casting pores in addition to further reducing the height. A direct cold rolling pass leads to cracking of the as cast sheets. After hot rolling the sheets were descaled by sandblasting and edged before being cold rolled at a four high rolling mill. The final thicknesses of 0.25, 0.27, and 0.3 mm were selected according to the industrial application and achieved with 3 to 5 rolling passes. Subsequently the sheets were cut to 100 mm x 100 mm with a wet-abrasive cut-off machine and annealed at temperatures between 740 °C and 980 °C, as shown in Fig. 8. In order to compare the strip-cast material with the industrial standard, a conventionally produced hot rolled strip of the same alloy with an initial thickness of 2 mm was cold rolled to the same final thicknesses in 5 to 6 passes and annealed in the equivalent manner.

Chemical composition. To account for potential deviations and impurities introduced during the production of the strip-cast material, the chemical composition of both the cast-strips and the

reference material was analyzed using spark emission spectroscopy. These analyses were performed on ground samples, cleaned with ethanol, using a BELEC Variolab spectrometer.

Microstructure and texture measurement. Samples for texture and optical investigations were extracted from the cast-strip, the rolled and the annealed samples, respectively. The microstructure evolution was characterized on RD-ND (rolling direction, normal direction) planes using an Olympus BX53 optical microscope after mechanical polishing and etching with an alcoholic 3 vol.% nitric acid solution (nital). The grain size was determined using a simple line measurement method based on DIN EN ISO 643 [12]. Where possible due to the microstructure, a sufficiently large measuring surface with a grain size of at least 50 grains was used. Texture measurements were conducted on RD-ND and TD-ND (transverse direction) planes by electron backscatter diffraction (EBSD) after mechanical and electrochemical polishing. Orientation data was acquired using a Hitachi SU5000 scanning electron microscope (SEM) equipped with a Nordlys detector from HKL Technology. Primary electron diffraction lines were generated using an acceleration voltage of 30 kV. Using the MTEX toolbox, a MATLAB-based software, the orientation distribution function (ODF) and texture index were estimated from the data.

Soft magnetic properties. To evaluate the magnetic properties, the final annealed sheets were analyzed using a single-sheet tester (SST). Measurements were performed with the MPG100 from Brockhaus, equipped with an SST sensor designed for 100 x 100 mm samples. Tests were conducted at frequencies of 400 Hz, and 1000 Hz. Power loss was measured at a polarization level of 1.0 T, as specified in the standards DIN EN 10106 and 10303. Maximum polarization was recorded for field strengths of 2,500 A/m, 5,000 A/m and 10,000 A/m. To ensure reproducibility, three samples of the same sheet thickness from a single annealing batch were measured, with values determined for both longitudinal and transverse directions.

Results and discussions

Chemical composition. The chemical compositions of the industrial hot rolled strip and the strip-cast sheet are presented in Table 1. Both materials show only minor differences in alloy content of the relevant elements, typically within a few hundredths. These variations are negligible, falling within the statistical measurement uncertainty of the device specifications. Therefore, any subsequent differences in processing or final properties cannot be attributed to variations in the basic chemical composition.

Table 1 – Chemical composition of the investigated industrial hot and cast-strip

	Si [wt.%]	Al [wt.%]	Mn [wt.%]
Industrial hot-strip	2.84	1.36	0.18
Strip-casted	2.89	1.34	0.19

Microstructure and Texture of Industrial Hot-Strip and As-Cast-strip. Fig. 2 compares the initial microstructures of the industrial hot rolled strip and the strip-cast sheet. The industrial hot rolled strip exhibits a finer, globular recrystallized microstructure near the strip surfaces, contrasting with a stretched and deformed central region aligned with the rolling direction. This uneven deformation is typical for hot rolling, where the majority of deformation energy is introduced in near-surface areas, promoting faster recrystallization. Due to static recrystallization during reheating in between rolling passes the overall microstructure can be described as fine. In contrast, the strip-cast material features globular grains in the central region and inward-oriented columnar grain structures starting from the surface, which have a significantly larger share of around two-thirds. The columnar grains typically exhibit an inclination of approximately 10° relative to the casting direction, a phenomenon also observed by Takatani et al. [13]. According to their findings,

this inclination results from the relative motion between the molten metal and the rotating casting gap formed by the casting rollers. As strip casting is typically followed by a hot rolling pass using the residual heat, the microstructure of the strip-cast material after a hot rolling pass with 20 % reduction is also compared to the initial microstructures. This process alters the microstructure, stretching individual grains and the overall grain structure further in the rolling direction as can be seen in Fig. 2 c). Additionally, the outer grain structure tilts in the rolling direction forming an angle of approximately 30° to a maximum of 45°. The original deviations caused by solidification during strip casting are entirely reversed during this step, facilitating the closure of solidification-related defects such as microvoids. However, recrystallization does not occur during the single hot rolling pass due to the absence of a phase transformation, insufficient deformation, and rapid air-cooling leading to a still coarse grain structure in comparison to the industrial hot-strip. A deviation of the microstructure after an actual inline hot rolling pass after strip casting cannot be ruled out, as the effects of reheating and rolling in the partially solidified state could not be simulated here.

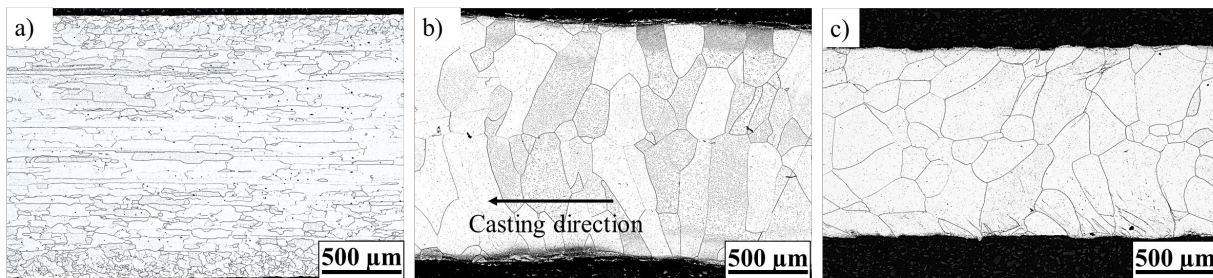


Figure 2 – Microstructure of a) industrial hot-strip with 2 mm thickness, b) as-cast-strip with 1.6 mm thickness and c) hot rolled cast-strip with 1.3 mm thickness

The initial textures of the materials differ significantly due to their respective manufacturing processes. As shown in the orientation distribution function (ODF) plots in Euler space, the industrial hot-strip exhibits a process-typical texture, characterized by a maximum at the $\{001\}<110>$ component and contributions from the Goss texture, see Fig. 3a). This texture, when considering magnetic anisotropy, is suboptimal for polarization. In contrast, the strip-cast material displays a distinct texture influenced by its solidification process [3]. As depicted in Fig. 3b), its maxima are located along the λ -fiber and within the Goss texture region, but with significantly lower intensity compared to the industrial hot-strip. After hot rolling of the strip casted sheets the texture aligns more with the texture of the industrial hot-strip. While the maxima distributions appear similar, the intensities in the hot rolled strip-cast material remain considerably weaker, see Fig. 3c). Notably, the strip-cast material lacks contributions from the Goss texture, instead exhibiting features closer to the γ -fiber. The weaker texture in the strip-cast material is likely attributable to its significantly reduced degree of rolling. For the material thicknesses used in this study, the reduction is approximately 20%, corresponding to a deformation degree of -0.29. In contrast, the industrial hot rolled strip undergoes substantially greater rolling and deformation during slab production, leading to higher deformation energy and a more pronounced texture development.

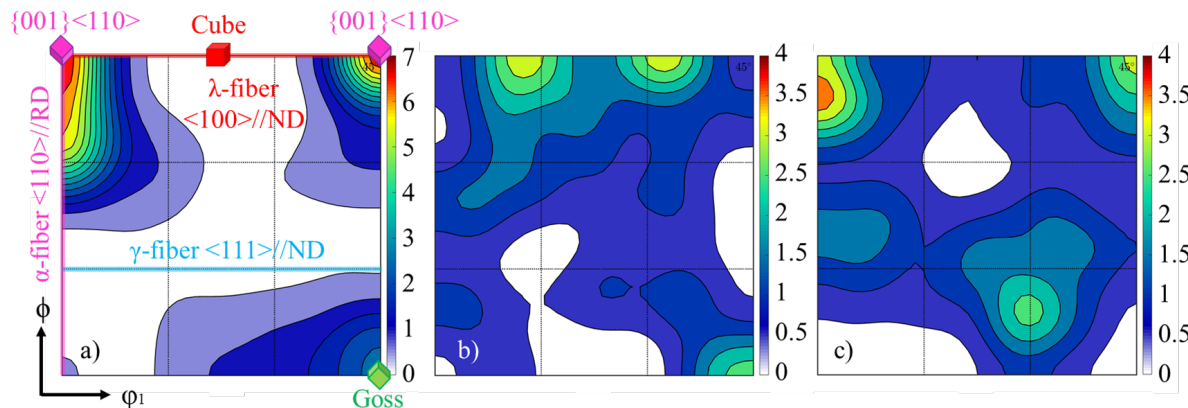


Figure 3 – Texture ($\phi_2 = 45^\circ$ ODFs) from a) industrial hot-strip, b) cast-strip, and c) hot rolled cast-strip with a reduction of 20 %

Microstructure and Texture evolution after cold-rolling. Fig. 4 shows the cold rolled microstructure of both the hot rolled and as-cast-strips, each characterized by typically elongated large grains. Consistent with the initial microstructure, the cold rolled strip-cast material exhibits coarser grains. The deformed microstructures are inhomogeneous and display notable differences depending on the prior processing route. Distinct “smooth” grains and “rough” grains with varying degrees of shear-bands are observed in the cold rolled sheets. Generally, greater deformation leads to an increased presence of grains with shear-bands and a higher density of shear-bands within grains [14]. In this study, a significantly greater number of grains with shear-bands are observed in the strip-cast material after cold rolling, despite it requiring a smaller reduction in height due to its lower initial thickness. This suggests that the influence of the initial microstructure outweighs the effects of deformation degree. It is well established that shear-band formation depends not only on cold rolling reduction but also on initial grain size and orientation. Paolinelli et al. [15] reported that a coarse grain size prior to cold rolling promotes shear-band formation, a finding consistent with the results of this study and those of Jiao et al. [3]. Another reason for the increased shear-band formation in strip casting material is the lower degree of dynamic recovery during hot rolling and the resulting lower stored energy of the grains. Additionally, both sheets demonstrate intense shear-band formation in the subsurface zone of the hot rolled samples with fewer shear-bands observed in the central grains. This might result from different texture across the sheet thickness. As shear-band formation is orientation-dependent, grains of differing orientations exhibit varying degrees of shear-bands under similar deformation conditions [14].

Fig. 5 presents the textures of hot-strip and strip-cast materials after cold rolling. The cold rolled hot-strip exhibits a texture characterized by a strong α -fiber, γ -fiber, and components of $\{001\}<110>$, with a pronounced peak at $\{112\}<110>$. In comparison, the cold rolled strip-cast material also shows strong α -fiber and γ -fiber components and the same texture maximum, but with significantly lower intensity. As observed after hot rolling, the reduced intensity is attributed to the lower degree of deformation in the strip-cast material.

Microstructure and Texture evolution after recrystallization. The recrystallization behavior of both investigated electrical steels, influenced by their initial properties, results in distinct recrystallization kinetics. The industrial reference material is examined first and shows fine recrystallized grains with a homogenous grain size. This material exhibits an expected recrystallization progression, as reflected in the subsequent grain size distributions. The cold rolling process introduces dislocations and shear-bands into the initial microstructure, promoting a more uniform recrystallization. Grain growth, while minimally dependent on annealing time under the constant duration used, is predominantly governed by the annealing temperature. Fig. 5 illustrates the kinetics of grain growth, which are critical for the final magnetic properties. It is

evident that as the annealing temperature increases, the grains become significantly coarser, with correspondingly increasing grain size.

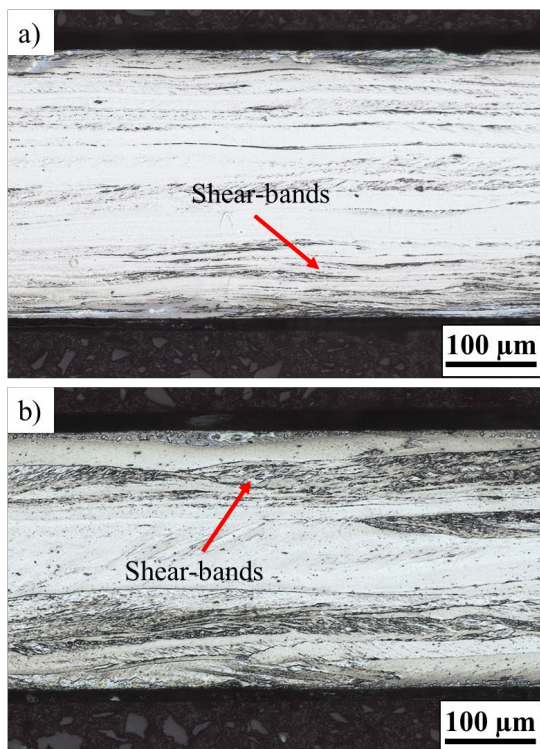


Figure 4 – Microstructure of cold rolled a) industrial hot-strip and b) cast-strip with 0.27 mm thickness

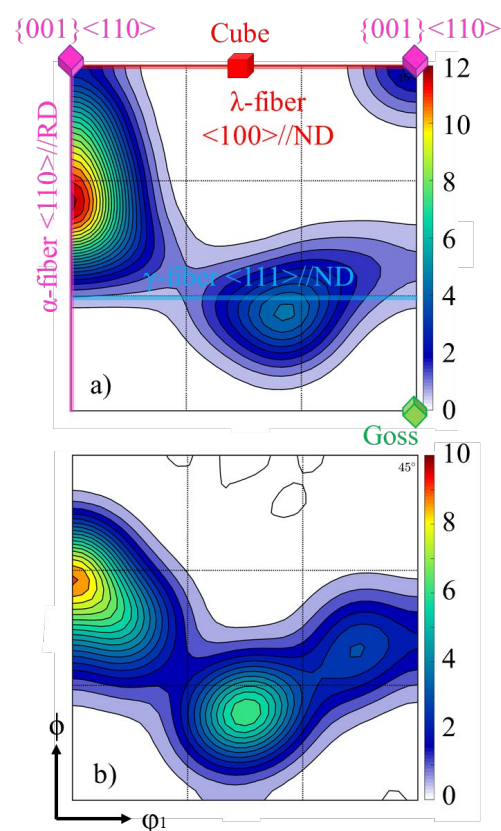


Figure 5 – Texture of cold rolled ($\phi_2 = 45^\circ$ ODFs) a) industrial hot-strip and b) cast-strip

The anticipated optimal grain size for magnetic properties, ranging from 40 μm to 80 μm , is achieved for the hot-strip at an annealing temperature of 860 $^\circ\text{C}$. Above 900 $^\circ\text{C}$, the grain size distribution noticeably broadens and deviates from a normal distribution. This effect, driven by the increased energy input at higher annealing temperatures, is further amplified by additional mechanisms. These mechanisms are also relevant to the strip-cast material and are discussed subsequently. The strip-cast material, characterized by a coarser and more inhomogeneous grain structure relatively to the hot-strip, exhibits altered recrystallization kinetics due to different shear-band concentrations in earlier processing steps. These differences lead to non-uniform recrystallization and irregular grain growth, as depicted in Fig. 6. As shown in Fig. 8 the strip-cast material initially displays a statistical normal grain size distribution at lower annealing temperatures. However, at temperatures above 820 $^\circ\text{C}$, the distribution flattens, and individual grain diameters exceeding 100 μm appear. Based on the resulting grain size, the optimal annealing temperature for the strip-cast material is determined to be between 820 $^\circ\text{C}$ and 860 $^\circ\text{C}$. After complete recrystallization and grain growth, the textures of the materials exhibit significant differences, as shown in Fig. 7. Both show a weakening of the α - and γ -fiber while the industrial reference material displays a more dominant texture near the α -fiber, resulting from cold rolling. In contrast, the strip-cast material shows its global maximum on the λ -fiber around the cube component, aligning with the direction of easiest magnetization, with only a local maximum near the α -fiber. Additionally, traces of the Goss texture or orientations nearby are still evident. These features reflect the influence of the initial texture of the strip-cast material, which also exhibited maxima along the λ -fiber and near the Goss orientation.



Figure 6 – Microstructure of cold rolled and annealed a) industrial hot-strip at 820 °C and b) cast-strip at 780 °C with 0.27 mm thickness

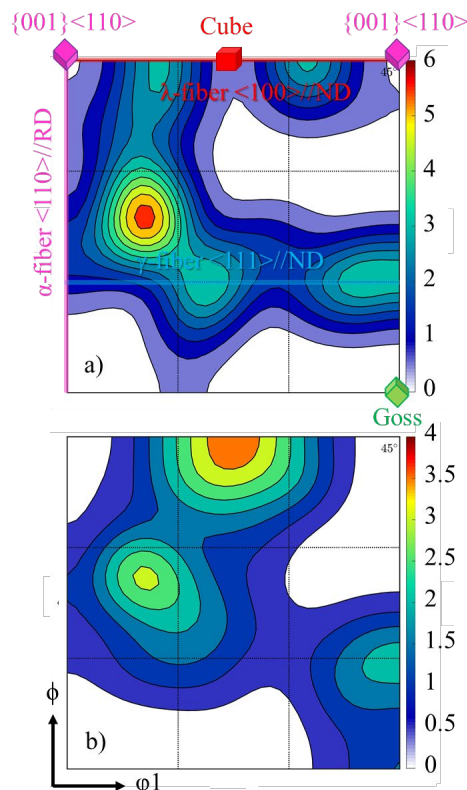


Figure 7 – Texture ($\phi_2 = 45^\circ$ ODFs) of annealed fully-finished a) industrial hot-strip and b) cast-strip

Magnetic properties. The results presented here are based on the application of materials in high-frequency electric machines, focusing on frequencies of 400 Hz and 1000 Hz at a maximum polarization of 1.0 T. Fig. 9 depicts the average polarization and core losses at different annealing temperatures for both the industrial reference material and the strip-cast material in their fully finished states. Measurements were conducted in longitudinal and transverse directions, and the values achieved meet the required specifications. Since polarization values showed minimal variation across different annealing temperatures, only the values at the optimal loss temperature are considered. The optimal grain size for minimizing core losses lies in the range of 40 to 80 μm , resulting from the distinct contributions of various loss mechanisms. The recrystallization kinetics of the materials, influenced by their initial properties, significantly affect the observed outcomes. For the hot-strip the magnetic properties confirm the findings regarding the material's optimal annealing conditions, identifying 860 °C as the ideal temperature. This annealing temperature corresponds to a mean grain size between 40 and 80 μm . At 860 °C, the material achieves a minimum core loss of 16.7 W/kg at 400 Hz. The corresponding polarization values are 1.55, 1.63, and 1.75 T for the respective field strengths. These results align with the anticipated behavior of the reference material. For the strip-cast material, the optimal annealing temperature based on grain size lies between 820 °C and 860 °C.

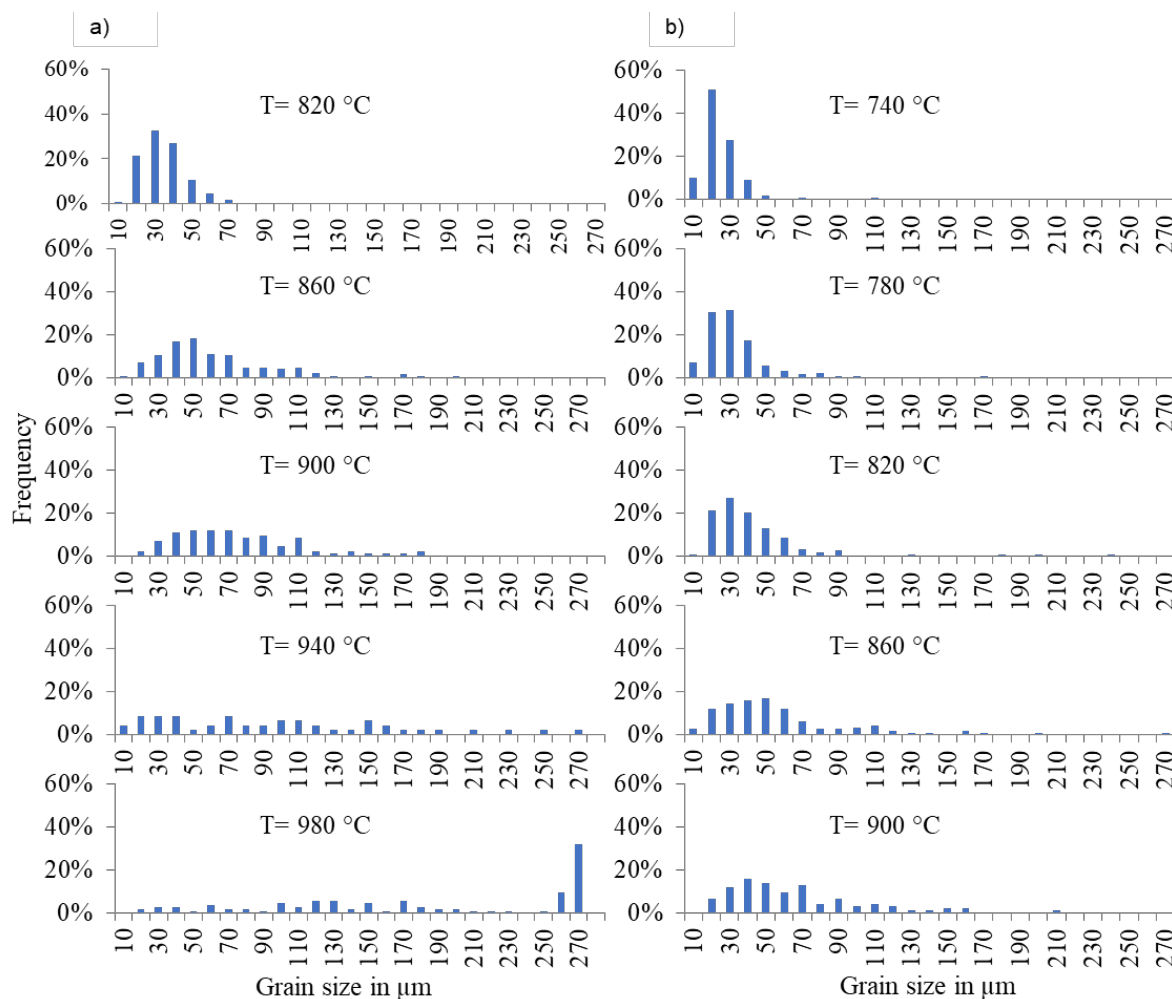


Figure 8 – Grain size distribution of cold rolled and annealed a) industrial hot-strip and b) cast-strip with 0.27 mm thickness for different annealing temperatures

However, when considering magnetic core losses, the optimal temperature shifts to 780 °C. This lower optimal temperature, approximately 80 °C below the reference material, is attributed to the broader grain size distribution. The inhomogeneous grain growth and uneven recrystallization kinetics prevent the grain size from being uniformly optimized leading to core loss values approximately 5–10% higher than the industrial reference material. Next to grain size this discrepancy may also partially stem from the descaling process. While the strip-cast material underwent sandblasting – leading to partially embedded and overlapping scale – the industrial reference material was pickled, resulting in a more thoroughly descaled surface. Conversely, the average polarization of the strip-cast material exceeds that of the reference material by approximately 0.03 T. These values remain well above the minimum required specifications. The superior polarization is primarily attributed to the magnetically favorable crystallographic texture of the strip-cast material. The initial texture, originating from the casting and solidification process, imparts favorable properties for maximum polarization especially the strong occupation of the λ -fiber. In subsequent rolling processes, the strip-cast material exhibits less pronounced rolling textures compared to the industrial reference, with the recrystallization texture closely resembling the primary texture. This phenomenon does not occur in the conventional production of the same alloy and contributes to the lower polarization values observed in the reference material.

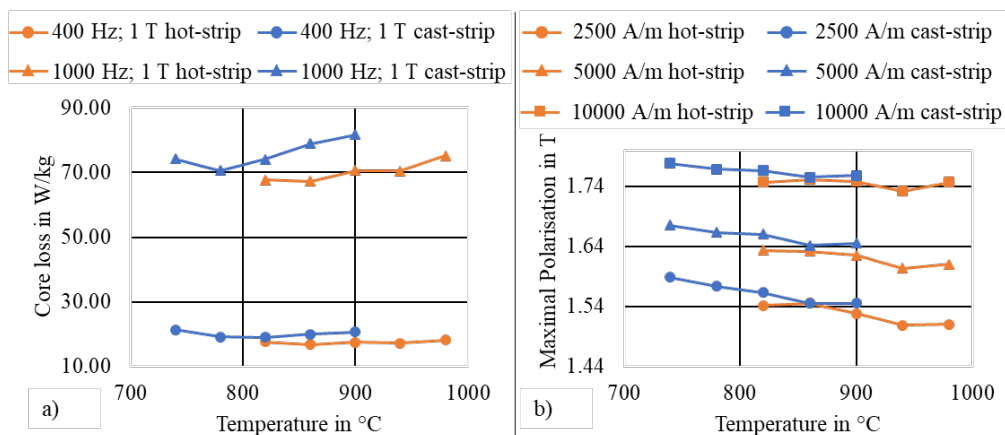


Figure 9 – Magnetic properties a) core losses and b) maximal polarization for the investigated materials after annealing

Summary

This study examines the microstructural and magnetic properties of non-grain-oriented (NGO) electrical steels produced via twin-roll casting (TRC) in comparison to conventionally hot-rolled Fe–2.9Si–1.35Al alloy. TRC enables the direct production of thin strips, significantly reducing energy consumption, costs, and emissions while promoting magnetically advantageous textures. The research explores the impact of subsequent processing steps, including hot rolling, cold rolling, and annealing, on microstructure, texture evolution, and magnetic performance. Key findings indicate that TRC produces columnar grain structures shaped by solidification dynamics and distinct λ -fiber textures, which enhance magnetic polarization by aligning crystallographic orientations along the easy magnetization axis. While these features result in higher average polarization compared to conventionally processed materials, challenges such as irregular recrystallization kinetics and non-uniform grain growth hinder grain size optimization and lead to slightly increased core losses. The study also reveals that while industrial hot-strip materials achieve optimal core losses at 860 °C, TRC materials require adjustments in annealing temperatures to attain comparable magnetic properties. This work emphasizes the potential of TRC to produce energy-efficient electrical steels and offers critical insights for optimizing processing parameters to enhance performance. Future research should focus on optimizing grain size by refining twin-roll casting (TRC) parameters, alloy composition, and thermal treatments to further enhance magnetic performance. In the alloying process, rare earth additions can facilitate grain refinement by influencing microstructural evolution, promoting a more homogeneous grain size distribution through tailored annealing treatments.

Acknowledgments

The authors would like to thank the Deutsche Forschungsgemeinschaft (DFG, German Research Foundation)—Projektnummer 432395971 for the financial support.

References

- [1] M. Ferry, *Direct strip casting of metals and alloys: Processing, microstructure and properties*, 1. Aufl. (Woodhead publishing in materials). Boca Raton, Fla., Cambridge: CRC Press; Woodhead, 2006
- [2] M. Müller, D. Bailly und G. Hirt, "Microstructure Evolution and Magnetic Properties of a 4.5 wt% Silicon Steel Produced by Twin-Roll Casting," *steel research int.*, Jg. 93, Nr. 11, 2022, Art. Nr. 2200554. <https://doi.org/10.1002/srin.202200554>

[3] H. Jiao *et al.*, "Significant effect of as-cast microstructure on texture evolution and magnetic properties of strip cast non-oriented silicon steel," *Journal of Materials Science & Technology*, Jg. 34, Nr. 12, S. 2472–2479, 2018. <https://doi.org/10.1016/j.jmst.2018.05.007>

[4] M. Gallaugher, P. Ghosh, A. M. Knight und R. R. Chromik, "The effect of easy axis misorientation on the low induction hysteresis properties of non-oriented electrical steels," *Journal of Magnetism and Magnetic Materials*, Jg. 382, S. 124–133, 2015. <https://doi.org/10.1016/j.jmmm.2015.01.067>

[5] L. Kestens und S. Jacobs, "Texture Control During the Manufacturing of Nonoriented Electrical Steels," *Texture, Stress, and Microstructure*, Jg. 2008, S. 1–9, 2008. <https://doi.org/10.1155/2008/173083>

[6] M. Mehdi, Y. He, E. J. Hilinski, L. A. Kestens und A. Edrisy, "The evolution of cube ($\{001\}<100>$) texture in non-oriented electrical steel," *Acta Materialia*, Jg. 185, S. 540–554, 2020. <https://doi.org/10.1016/j.actamat.2019.12.024>

[7] Y. H. Sha *et al.*, "Strong cube recrystallization texture in silicon steel by twin-roll casting process," *Acta Materialia*, Jg. 76, S. 106–117, 2014. <https://doi.org/10.1016/j.actamat.2014.05.020>

[8] E. Stephenson und A. Marder, "The effects of grain size on the core loss and permeability of motor lamination steel," *IEEE Trans. Magn.*, Jg. 22, Nr. 2, S. 101–106, 1986. <https://doi.org/10.1109/tmag.1986.1064281>

[9] N. Leuning, S. Steentjes und K. Hameyer, "Effect of grain size and magnetic texture on iron-loss components in NO electrical steel at different frequencies," *Journal of Magnetism and Magnetic Materials*, Jg. 469, S. 373–382, 2019. <https://doi.org/10.1016/j.jmmm.2018.07.073>

[10] H. Jiao *et al.*, "Role of Hot Rolling in Microstructure and Texture Development of Strip Cast Non-Oriented Electrical Steel," *Metals*, Jg. 12, Nr. 2, S. 354, 2022. <https://doi.org/10.3390/met12020354>

[11] M. Daamen, B. Wietbrock, S. Richter und G. Hirt, "Strip Casting of a High-Manganese Steel (FeMn22C0.6) Compared with a Process Chain Consisting of Ingot Casting and Hot Forming," *steel research int.*, Jg. 82, Nr. 1, S. 70–75, 2011. <https://doi.org/10.1002/srin.201000267>

[12] DIN EN ISO 643:2020-06, *Stahl - Mikrophotographische Bestimmung der erkennbaren Korngröße (ISO_643:2019, korrigierte Fassung 2020-03); Deutsche Fassung ISO_643:2020*, Berlin

[13] H. Takatani, C.-A. Gandin und M. Rappaz, "EBSD characterisation and modelling of columnar dendritic grains growing in the presence of fluid flow," *Acta Materialia*, Jg. 48, Nr. 3, S. 675–688, 2000. [https://doi.org/10.1016/S1359-6454\(99\)00413-9](https://doi.org/10.1016/S1359-6454(99)00413-9)

[14] M. L. Lobanov, G. M. Rusakov, A. A. Redikul'tsev, M. S. Karabanalov und L. V. Lobanova, "Shear bands in Fe-3% Si-0.5% Cu alloy," *Steel Transl.*, Jg. 41, Nr. 7, S. 559–564, 2011. <https://doi.org/10.3103/S0967091211070060>

[15] S. C. Da Paolinelli, M. A. Da Cunha und A. B. Cota, "The influence of shear bands on final structure and magnetic properties of 3% Si non-oriented silicon steel," *Journal of Magnetism and Magnetic Materials*, Jg. 320, Nr. 20, e641-e644, 2008. <https://doi.org/10.1016/j.jmmm.2008.04.050>